

ICEPP Report 02-01
20 June 2001

Topology-oriented Searches for Supersymmetric Particles at LEP

Shoji ASAI

*International Centre for Elementary Particle Physics, University of Tokyo,
7-3-1 Bunkyo-ku, Hongo, Tokyo 113, Japan
E-mail Shoji.Asai@cern.ch*

Abstract

Searches for various new particles and phenomena are performed at LEP with data collected at \sqrt{s} upto 209 GeV. Topology-oriented studies have been performed, and almost all possible topologies are covered. No interesting excess above 2.5σ was found. The results on supersymmetric particles are summarised.

This note contributes to proceedings of Lathuile 2001

1 Introduction

The LEP e^+e^- collider was operated at the centre-of-mass energies, \sqrt{s} , of 189, 192-202 and 202-209 GeV¹ for the last three years. Each of the four LEP experiments, ALEPH, DELPHI, L3 and OPAL collected integrated luminosities of about 180, 220 and 220 pb⁻¹ at 189, 192-202 and 202-209 GeV, respectively. Using these data samples at highest energies and with significant luminosities, searches for various new particles and phenomena have been performed. In this note, the results on supersymmetric particles are summarised. In section 3, new result using data corrected at Z^0 -pole is reported to search for the light gluino \tilde{g} .

The supersymmetric (SUSY) standard models are most promising extensions of the standard model, because the SUSY can naturally deal with the problem of the quadratic Higgs mass divergence. In these theories, each elementary particle has a superpartner whose spin differs by 1/2 from that of the particle. Although there are, in general, more than 100 free parameters to describe SUSY soft breaking, three predictable and promising SUSY models are listed here.

- Gravity Mediated Model(called “CMSSM” thereafter);
 - (1) There are only five parameters after imposing GUTs conditions, $\tan\beta(\equiv v_2/v_1)$, M_2 (SU(2) gaugino mass), μ (superpotential Higgs mass), m_0 (universal scalar mass), and A (scalar trilinear coupling).
 - (2) The lightest supersymmetric particle (LSP) is the lightest neutralino, $\tilde{\chi}_1^0$.
 - (3) The promising signals at LEP are $\tilde{\chi}_1^+\tilde{\chi}_1^-$, $\tilde{\chi}_1^0\tilde{\chi}_2^0$, $\tilde{\ell}^+\tilde{\ell}^-$, $\tilde{t}_1\tilde{t}_1$ and $\tilde{b}_1\tilde{b}_1$.
 - (4) Missing transverse energy, \cancel{E}_T , carried away by $\tilde{\chi}_1^0$'s is the experimental signature, if R-parity [?] is conserved. R-parity is defined to be even for the ordinary particles and odd for the superpartners($R \equiv (-1)^{2S+3B+L}$). When R-parity is conserved, SUSY particles should be produced in pairs, the lightest SUSY particle (LSP) should be stable.

¹The highest \sqrt{s} is 209 GeV, but the integrated luminosity at this \sqrt{s} is very small. The highest \sqrt{s} with the reasonable luminosity is 207 GeV.

Other SUSY particles should decay finally into the LSP and ordinary particles.

- Gauge Mediated Model(called “GMSB” thereafter);
 - (1) There are five parameters as follows; \sqrt{F} (SUSY breaking scale), M_m (mass of messenger sector), Λ (SUSY particle mass), sign of μ and $\tan\beta$. (2) The LSP is gravitino, \tilde{G} , whose mass is expected to be smaller than a few KeV. (3) \cancel{E}_T carried by \tilde{G} 's and photons the experimental signature. (4) The next lightest supersymmetric particle (NLSP) is $\tilde{\ell}$ or $\tilde{\chi}_1^0$, then the promising signals at LEP are $\tilde{\ell}^+\tilde{\ell}^-$ and $\tilde{\chi}_1^0\tilde{\chi}_1^0$.
- Anomary Mediated Model(called “AMSB” thereafter);

Parameters are the same as in MSSM, but Wino mass at electro-weak scale is very close to Bino mass, then the mass difference between $\tilde{\chi}_1^\pm$ and $\tilde{\chi}_1^0$ is very small.

These models are used to guide the analyses but more general cases are studied. Searches at LEP can be performed independently from these specific models, since e^+e^- annihilation is very clean, and since the almost all background processes are well simulated at LEP. We have performed “*topology-oriented studies*”. The interesting topologies are picked up, and various distributions are compared with expectations of the standard model processes. After these careful comparisons, interpretations have been performed using these models. The promising event topologies, which are reported in this note, are listed in table 1. The other interesting topologies, for example mono-jet, are also studied at LEP, but are not mentioned in the note.

The production cross-section of $\tilde{\chi}_1^+\tilde{\chi}_1^-$, $\tilde{\chi}_1^0\tilde{\chi}_2^0$ and $\tilde{f}^+\tilde{f}^-$ are typically about $(1 - 10)\beta$ pb, $(0.2 - 2)\beta$ pb and $(0.2 - 2)\beta^3$ pb, respectively. The β is the velocity of the produced SUSY particles, which is determined by these masses and \sqrt{s} . Precise values of the cross-sections and decay branching fraction depend on the SUSY parameters. On the other hand, the sources

Table 1: *The promising Event topologies of SUSY signal. \circ indicates “very promising” and Δ “possible and interesting topology”*

Event topology	CMSSM	GMSB	AMSB
One or two $\gamma + \cancel{E}_T$	Δ $\tilde{\chi}_1^0 \tilde{\chi}_2^0 (\rightarrow \tilde{\chi}_1^0 \gamma)$	\circ $\tilde{\chi}_1^0 \tilde{\chi}_1^0 (\rightarrow \tilde{G} \gamma \tilde{G} \gamma)$ $\tilde{\chi}_1^0 \tilde{G} (\rightarrow \tilde{G} \gamma \tilde{G})$	
Acoplaner leptons + \cancel{E}_T	\circ $\tilde{\ell}^+ \tilde{\ell}^- (\rightarrow \ell \tilde{\chi}_1^0 \ell \tilde{\chi}_1^0)$	\circ $\tilde{\ell}^+ \tilde{\ell}^- (\rightarrow \tilde{G} \ell \tilde{G} \ell)$	
Acoplaner jet pair + \cancel{E}_T	\circ $\tilde{t}_1 \tilde{t}_1, \tilde{b}_1 \tilde{b}_1, \tilde{\chi}_1^0 \tilde{\chi}_2^0$		
Long-lived heavy particles	Δ $\tilde{\chi}_1^+ \tilde{\chi}_1^-, \tilde{\ell}^+ \tilde{\ell}^-$ very small ΔM	\circ $\tilde{\ell}^+ \tilde{\ell}^-$ large \sqrt{F}	\circ $\tilde{\chi}_1^+ \tilde{\chi}_1^-$
$W^+ W^- / Z$ -like + \cancel{E}_T	\circ $\tilde{\chi}_1^+ \tilde{\chi}_1^-, \tilde{\chi}_1^0 \tilde{\chi}_2^0,$		
$\gamma + X + \cancel{E}_T$	Δ $\tilde{\chi}_1^+ \tilde{\chi}_1^- \gamma (\text{ISR})$ small ΔM	Δ $\tilde{\chi}_1^+ \tilde{\chi}_1^-, \tilde{\chi}_1^0 \tilde{\chi}_2^0,$ $(\tilde{\chi}_1^0 \rightarrow \gamma \tilde{G})$	\circ $\tilde{\chi}_1^+ \tilde{\chi}_1^- \gamma (\text{ISR})$
Many leptons plus jets	\circ R-violated		\circ R-violated

of background to these signals are two-photon, lepton pairs, multihadronic, photonic and four-fermion processes. Two-photon processes are the most important background for the case of small ΔM , where the visible energy and momentum transverse to the beam direction for signal and two-photon events are comparatively small. The production cross-section in hadronic final state of the processes is about 10^4 pb, in which invariant mass of the hadronic system is larger than 5 GeV. Four-fermion processes, W^+W^- , $We\nu$, γ^*Z and $ZZ^{(*)}$, are the most significant background for the case of large ΔM . The W^+W^- process, which have topologies very similar to that of the $\tilde{\chi}_1^+\tilde{\chi}_1^-$ are dominant contributions of four-fermion. The cross-section is about 17 pb.

2 Results on various topologies

2.1 One or two γ with missing transverse energy

Event topology consisting of single or two photons with large E_T arise in various of models, especially in the GMSB model. For example, $\tilde{\chi}_1^0\tilde{\chi}_1^0$ is pair-produced through the \tilde{e} -exchange (t -channel), and $\tilde{\chi}_1^0$ decays into $\gamma\tilde{G}$. This process gives topology of two γ 's with E_T . Photonic signature can also be important in the CMSSM, when the radiative decay $\tilde{\chi}_2^0 \rightarrow \tilde{\chi}_1^0\gamma$ is dominant.

These new physics contributions to these topologies have an irreducible background from the Standard Model process $e^+e^- \rightarrow \nu\bar{\nu}\gamma(\gamma)$. However, such contributions can potentially be distinguished from the background by examination of the mass of the system recoiling against the selected photon system which, for the Standard Model process, is dominantly peaked at the mass of the Z^0 .

Figures 1 show the LEP-combined distributions of the recoil mass for one or two photon events with large E_T . As shown in these figures, there are generally good agreements between the data and the expectation from

the Standard Model in both topologies² No anomalous production of these topologies has been observed. Various interpretations have been performed within various models. Figure 2 shows the excluded region in $(M_{\tilde{e}}, M_{\tilde{\chi}_1^0})$ plane in the GMSB model. As shown in this figure, lower-limit on $\tilde{\chi}_1^0$ mass is 95 GeV, when \tilde{e} is lighter than 200 GeV. The hypothesis that the interesting event of $e^+e^- \gamma\gamma$ with \cancel{E}_T observed at CDF is considered as the GMSM signal is ruled out.

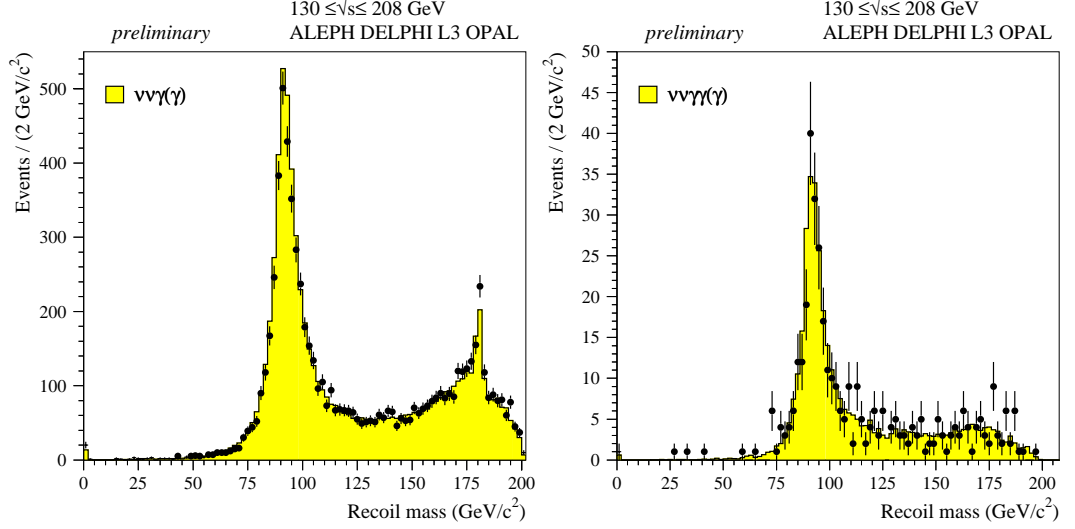


Figure 1: Recoil mass distribution for the single γ topology (Left) and two γ 's with \cancel{E}_T topology (Right). Data is shown by the points with error bars and hatched histogram show the predictions for the process of $\nu\bar{\nu}\gamma(\gamma)$.

2.2 Acoplanar lepton pair

Acoplanar lepton pair is good signal of scalar leptons. On the other hand W^+W^- and $e^+e^- \ell^+\ell^-$ processes dominantly provide events of this topology in the Standard Model. Scalar leptons could be pair-produced through γ or Z^0 exchange processes (s -channel). Scalar electrons (\tilde{e}) could also be

²Deficit of $(5.4 \pm 1.5 \%)$ was found at M_Z in the single γ topology, and it does not have \sqrt{s} -dependence. It might be due to Koralz generator which is mainly used to estimate $e^+e^- \rightarrow \nu\bar{\nu}\gamma\gamma$ processes. This deficit becomes small if NUNUGPV generator, which is made specially for this process, was used, but still under investigating.

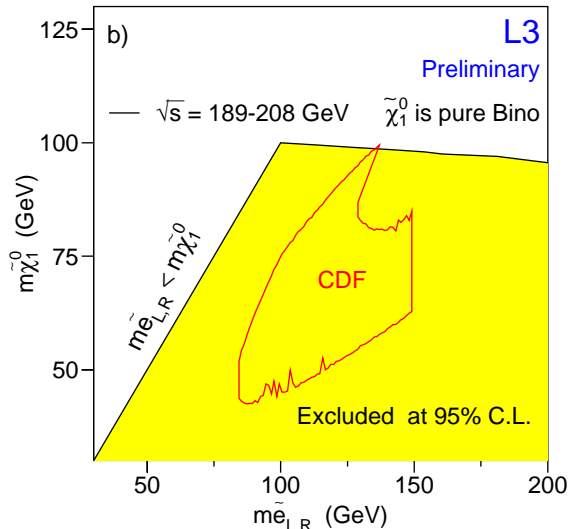


Figure 2: Excluded regions in $(M_{\tilde{e}_R}, M_{\tilde{\chi}_1^0})$ plane.

produced through t -channel neutralino exchange enhancing the production cross-section compared to those for the other sleptons. Each lepton has two scalar partners, the right- and left-handed scalar leptons ($\tilde{\ell}_R$ and $\tilde{\ell}_L$), according to the helicity states of their non-SUSY partners. In general the cross-sections for right-handed sleptons are smaller than for left-handed, so only the right-handed sleptons are considered here.

Slepton decay dominantly into a lepton and the $\tilde{\chi}_1^0(\tilde{G})$ in CMSSM(GMSB), appearing in the detector as a pair of acoplanar lepton pairs. If the second lightest neutralino, $\tilde{\chi}_2^0$, is lighter than sleptons, cascade decay is also possible in CMSSM.

No excess was observed in this topology at all four experiments³ Figures 3 show the LEP combined results on the excluded regions in $(M_{\tilde{\ell}}, M_{\tilde{\chi}_1^0})$ for each flavour in CMSSM frame. The cross-section of \tilde{e}_R and branching fraction of the cascade decay are calculated with the MSSM model, in which $\tan\beta=1.5$

³Excess larger than 3σ was observed in acoplanar τ pair at $\sqrt{s}=189$ and $192-202$ GeV. This was consistent with the $\tilde{\tau}$ signal ($m(\tilde{\tau}) = 85$ GeV and $m(\tilde{\chi}_1^0)=22$ GeV). But this excess was not confirmed in the highest energy data at $\sqrt{s}=202-209$ GeV. The excess was reduced to 2σ , if data for the last 3 years were combined

and $\mu=-200$ GeV are chosen. The lower-limits on $M_{\tilde{\ell}}$ are 98 GeV for \tilde{e}_R and 93 GeV for $\tilde{\mu}_R$, if $\Delta M(\equiv M_{\tilde{\ell}} - M_{\tilde{\chi}_1^0})$ is larger than 3 GeV. The lower-limits on $M_{\tilde{\tau}}$ is, a little bit worse due to the small excess mentioned in the footnote, 80 GeV if ΔM is larger than 10 GeV.

Using the results on acoplanar lepton pair and on two γ 's with \cancel{E}_T energy, we can derive absolute lower-limit in the GMSB model. Figure 4 shows the 95% C.L. excluded regions in $M_{\tilde{\chi}_1^0}$ versus $M_{\tilde{\tau}}$. Small $M_{\tilde{\chi}_1^0}$ region is covered by $\tilde{\chi}^0 1 \tilde{\chi}^0 1 \rightarrow \gamma \tilde{G} \gamma \tilde{G}$, and the region of small $M_{\tilde{\tau}}$ is covered by $\tilde{\ell}^+ \tilde{\ell}^- \rightarrow \ell \tilde{G} \ell \tilde{G}$. Cross point of these regions gives the absolute lower-limits [?], which are $M_{\tilde{\tau}} \geq 83$ GeV and $M_{\tilde{\chi}_1^0} \geq 85$ GeV for $\tan\beta=2$. As $\tan\beta$ is larger, mass difference between $\tilde{\tau}$ and $\tilde{\mu}$ becomes large, due to mixing effect of the Left-Right handed state. The Lower-limits are $M_{\tilde{\tau}} \geq 69$ GeV and $M_{\tilde{\chi}_1^0} \geq 76$ GeV in this case. Data at $\sqrt{s} \geq 190$ GeV have not yet included to calculate these values.

2.3 Acoplanar jet pair

Acoplanar jet pair events with \cancel{E}_T are interesting topology to study the four-fermion processes. Events with this topology mainly come from the following four-fermion processes.

- (1) $Z^0 \gamma^* \rightarrow \nu \nu q \bar{q}$ or $Z^0 Z^* \rightarrow \nu \nu q \bar{q}$: Two peaks are expected in visible mass, M_{vis} , distribution at 0 and M_Z as shown in Fig. 5.
- (2) $W e \nu \rightarrow e \nu q \bar{q}$, in which the electron escapes into beam pipe: Peak appears in M_{vis} distribution at M_W .
- (3) $e^+ e^- \rightarrow e \nu q \bar{q}$, through the multi-peripheral diagram. Since the photon is quasi on-shell, the electron escapes into beam pipe. The invariant mass of $q \bar{q}$ becomes smaller than M_W .

This topology is also the signal of the new physics processes of neutralino or scalar quarks, especially squarks of third generation. The scalar top quark (\tilde{t}), the bosonic partner of the top quark, can be the lightest charged

SUSY particle for two reasons. Firstly, one loop radiative corrections to the \tilde{t} mass through Higgsino-quark loops and Higgs-squark loops are always negative. The correction is large for a large top quark mass. Secondly, the supersymmetric partners of the left-handed and right-handed top quarks (\tilde{t}_L and \tilde{t}_R) mix, and the resultant two mass eigenstates (\tilde{t}_1 and \tilde{t}_2) have a large mass splitting. The lighter mass eigenstate ($\tilde{t}_1 = \tilde{t}_L \cos(\theta_{\tilde{t}}) + \tilde{t}_R \sin(\theta_{\tilde{t}})$) can be lighter than any other charged SUSY particle. The $\theta_{\tilde{t}}$ can be determined by the top quark mass and the SUSY parameters in the CMSSM. In the case with the large $\tan\beta$, the scalar bottom quark (\tilde{b}) can be light for the similar reasons to \tilde{t} . The lighter mass eigenstate(\tilde{b}_1) of \tilde{b} is also the mixing state of \tilde{b}_L and \tilde{b}_R , *i.e.* $\tilde{b}_1 = \tilde{b}_L \cos(\theta_{\tilde{b}}) + \tilde{b}_R \sin(\theta_{\tilde{b}})$.

The $\tilde{t}_1(\tilde{b}_1)$ is pair-produced through γ or Z^0 exchange processes. If the $\theta_{\tilde{t}}=56^\circ$ ($\theta_{\tilde{b}}=68^\circ$), the \tilde{t}_1 (\tilde{b}_1) decouples from Z^0 , and the production cross-section becomes small. Because the lifetime of the \tilde{t}_1 is much longer than the typical time scale of the hadronisation the \tilde{t}_1 would hadronise to form a \tilde{t}_1 -hadron before it decays. The experimental signature for $\tilde{t}_1\tilde{t}_1$ events is an acoplanar sharp two-jet topology with large transverse momentum. The \tilde{b}_1 decays dominantly into b-quark and the $\tilde{\chi}_1^0$, appearing in the detector as an acoplanar two-jet.

No excess was found in acoplanar two-jet topology and the LEP-combined limits on \tilde{t}_1 and \tilde{b}_1 are shown in Fig. 6. The lower-limit on \tilde{t}_1 -mass is 93 GeV even for decoupling case, if the \tilde{t}_1 decays into $c\tilde{\chi}_1^0$, and the mass difference between \tilde{t}_1 and $\tilde{\chi}_1^0$ is larger than 5 GeV. The \tilde{b}_1 -mass limit is 92 GeV, if the mass difference between the \tilde{b}_1 and $\tilde{\chi}_1^0$ is larger than 10 GeV.

2.4 Long-lived heavy particles

The coupling of \tilde{G} is propotional to \sqrt{F}^{-1} . When \sqrt{F} is larger than $O(100TeV)$ in the GMSB model, lifetime of $\tilde{\ell}$ is sizable, *i.e* the decay point of $\tilde{\ell}$ is far from the vertex point (Type-I) or the outside of the detector(Type-II). Forthermore $\tilde{\chi}_1^\pm$ can not decay in the detectors(Type-II), when the mass difference between $\tilde{\chi}_1^\pm$ and $\tilde{\chi}_1^0$ is smaller than 100 MeV in the CMSSM and

AMSB models. The experimental signatures are large IP track or kink track for Type-I and heavy stable particle for Type-II. Heavy particles are searched for using the energy-loss measurements in the central tracking system (dE/dx) and particle ID informations (for example, using RICH counters).

No evidence was observed in all the experiments, and many interpretations have been performed in various models. For example, Fig 7 shows the lower-limit on $M_{\tilde{\tau}_1}$ as function of $M_{\tilde{G}}$ in the GMSB model. Mass of \tilde{G} is proportional to \sqrt{F} . Region of $M_{\tilde{G}} \leq O(1)$ eV, in which coupling of \tilde{G} is comparable with the weak coupling, should be covered by study on the acoplanar lepton pair. Lifetime of $\tilde{\ell}^+\tilde{\ell}^-$ becomes much longer than 10^{-8} sec (Type-II), and $\tilde{\ell}$ plays as heavy stable particles in detectors, when $M_{\tilde{G}}$ is heavier than $O(100)$ eV. In intermediate case ($M_{\tilde{G}} \sim O(1-100)$ eV), $\tilde{\ell}$ decays far from vertex, in which ℓ -track should be observed as large IP track or kink track.

2.5 W^+W^-/\mathbf{Z} -like + missing transverse energy

Evidence of chargino and neutralino is definite signal of the SUSY models, and many effort have been made toward searches for them at LEP. $\tilde{\chi}_i^\pm$, are the mass eigenstates formed by the mixing of the fields of the fermionic partners of the charged gauge bosons (winos) and those of the charged Higgs bosons (charged higgsinos). Fermionic partners of the γ , the Z boson, and the neutral Higgs bosons mix to form the mass eigenstates called neutralinos, $\tilde{\chi}_j^0$ ⁴.

$\tilde{\chi}_1^+\tilde{\chi}_1^-$ are pair-produced through γ - or Z-exchange in the s -channel, if kinematically possible. For the wino component, there is an additional production process through scalar electron-neutrino ($\tilde{\nu}_e$) exchange in the t -channel. The production cross-section is large unless the scalar neutrino ($\tilde{\nu}$) is light, in which case the cross-section is reduced by destructive interference between the s -channel and t -channel diagrams. $\tilde{\chi}_1^+$ decays dominantly

⁴In each case, the index $i = 1, 2$ or $j = 1$ to 4 is ordered by increasing mass.

into $\tilde{\chi}_1^0 \ell^+ \nu$ or $\tilde{\chi}_1^0 q \bar{q}'$ via a virtual W boson in much of the parameter space. Then $W^+ W^-$ -like events with \cancel{E}_T carried by $\tilde{\chi}_1^0$ is interesting and important topology for $\tilde{\chi}_1^+ \tilde{\chi}_1^-$. For small scalar lepton masses, decays to leptons become important. The details of chargino decay and production cross-section depend on the parameters of the mixing of wino and higgsino and the masses of $\tilde{\nu}$ and $\tilde{\ell}$ in the CMSSM model.

Neutralino pairs ($\tilde{\chi}_1^0 \tilde{\chi}_2^0$) can be produced through a virtual Z (s -channel) or by a scalar electron (t -channel) exchange. The $\tilde{\chi}_2^0$ will decay into $\tilde{\chi}_1^0 \nu \bar{\nu}$, $\tilde{\chi}_1^0 \ell^+ \ell^-$ or $\tilde{\chi}_1^0 q \bar{q}$ through a virtual Z boson, sneutrino, slepton, squark or a neutral SUSY Higgs boson (h^0 or A^0). Since the decay via a virtual Z is the dominant mode in most of the parameter space, the Z^0 -like event with \cancel{E}_T is characteristic and important topology of $\tilde{\chi}_1^0 \tilde{\chi}_2^0$ signal.

No excess was found and Fig. 8 show model-independent upper-limits (95% C.L.) on the production cross-sections of $\tilde{\chi}_1^+ \tilde{\chi}_1^-$ and $\tilde{\chi}_2^0 \tilde{\chi}_1^0$. These are obtained assuming the decay mode $\tilde{\chi}_1^\pm \rightarrow \tilde{\chi}_1^0 W^{(*)}$ for $\tilde{\chi}_1^+ \tilde{\chi}_1^-$, and $\tilde{\chi}_2^0 \rightarrow \tilde{\chi}_1^0 Z^{(*)}$ for $\tilde{\chi}_1^+ \tilde{\chi}_2^0$ production. If the cross-section for $\tilde{\chi}_1^+ \tilde{\chi}_1^-$ is larger than 0.6 pb and ΔM between $\tilde{\chi}_1^+$ and $\tilde{\chi}_1^0$ is between 5 GeV and about 80 GeV, $\tilde{\chi}_1^\pm$ is excluded almost up to the kinematic limit as shown in Fig. 8. More strict limits are obtained for $\tilde{\chi}_1^0 \tilde{\chi}_2^0$ production.

As mentioned above, cross-sections and decay branching fractions of $\tilde{\chi}_1^+ \tilde{\chi}_1^-$ and $\tilde{\chi}_1^0 \tilde{\chi}_2^0$ depend on the SUSY parameters, especially on the scalar lepton mass, in CMSSM. Light $\tilde{\nu}$ gives the small cross-section of $\tilde{\chi}_1^+ \tilde{\chi}_1^-$ and large branching fraction of $\tilde{\chi}_1^+$ into $\ell \nu \tilde{\chi}_1^0$. Figure 2.5(a) shows the lower-limit on $M_{\tilde{\chi}_1^\pm}$ as function of $M_{\tilde{\nu}}$. The lower-limit on $M_{\tilde{\chi}_1^\pm}$ is 103.5 GeV, if $\tilde{\nu}$ is heavier than 300 GeV, $\mu = -200$ GeV, and $\tan \beta = 2$. More general case, lower-limit is 98.6 GeV (DELPHI, *preliminary*) for all parameters in CMSSM.

These limits on $\tilde{\chi}_1^+ \tilde{\chi}_1^-$, $\tilde{\chi}_1^0 \tilde{\chi}_2^0$, and $\tilde{\ell}^+ \tilde{\ell}^-$ can be also interpreted into $\tilde{\chi}_1^0$ mass in the CMSSM. This has implications for direct searches for the lightest neutralino as a candidate for dark matter. Figure 2.5(b) shows the dependence of the mass limits on the value of $\tan \beta$. Of particular

interest is the absolute lower limit on the mass of the lightest neutralino of $m_{\tilde{\chi}_1^0} > 38.7$ GeV (36.7 GeV) at 95% C.L. for $m_0 \geq 1000$ GeV (all m_0).

2.6 γ +some activity with missing transverse energy

Studies reported in section 2.5 are based on the visible particles emitted from decays of $\tilde{\chi}_1^\pm$. When the mass difference between $\tilde{\chi}_1^\pm$ and $\tilde{\chi}_1^0$ is smaller than 3 GeV, these emitted particles are too soft to trigger and to be studied, since cross-section of the two-photon processes are huge in such a region of very low energy. Initial state radiation photon (ISR γ) helps to study such a degeneration case. The analysis is based on the reconstruction of the isolated ISR γ together with the low-momentum detectable decay products. The ISR γ photons are required to have enough transverse momentum (7 GeV^5) with respect to the beam pipe to ensure the trigger.

No excess was found in this topology, and the limit is interpreted into chargino mass in the CMSSM and AMSB models. Figure 9 shows lower-limits on chargino mass as function of mass difference. Study on this topology covers region of $\Delta M=2 \text{ GeV}-M_\pi$. When the mass difference is smaller than M_π , chargino can not decay in the detectors. This case is covered by the study of heavy stable particles. Absolute lower-limit is 89.5 GeV in the CMSSM (ALEPH, *preliminary*).

2.7 Many leptons plus jets

The lightest neutralino $\tilde{\chi}_1^0$ will decay and the topologies differ significantly from the previous sections, if R-parity is not conserved. Violating interactions are, in general, parametrised with a gauge-invariant super-potential that includes the following Yukawa coupling terms:

$$W_{RPV} = \lambda_{ijk} L_i L_j \bar{E}_k + \lambda'_{ijk} L_i Q_j \bar{D}_k + \lambda''_{ijk} \bar{U}_i \bar{D}_j \bar{D}_k, \quad (1)$$

where i, j, k are the generation indices of the super-fields L, Q, E, D and U . L and Q are lepton and quark left-handed doublets, respectively. \bar{E}, \bar{D} and \bar{U}

⁵depending on \sqrt{s}

Table 2: Possible event topologies of $\tilde{\chi}_1^+ \tilde{\chi}_1^-$ event with R -parity violation.

	without \cancel{E}_T	with \cancel{E}_T
λ_{ijk}	6ℓ	$2\ell, 4\ell, 6\ell,$ $4q+4\ell, 4q+5\ell$
λ'_{ijk}	$4q+2\ell,$ $8q+2\ell$	$4q, 4q+\ell, 4q+2\ell, 4q+3\ell, 4q+4\ell,$ $6q+\ell, 6q+2\ell, 6q+3\ell,$ $8q, 8q+\ell$
λ''_{ijk}	$6q,$ $10q$	$6q+2\ell,$ $8q+\ell$

are right-handed singlet charge-conjugate super-fields for the charged leptons and down- and up-type quarks, respectively. Due to these interactions $\tilde{\chi}_1^0$ can decay into three standard fermions, whose generations are determined by the lagragian (1). $\tilde{\chi}_1^\pm$ also can decay into three standard fermions through these intereactions. Various topologies are possible as shown in Table 2, and almost all these topologies have been studied at LEP. $\tilde{f}\tilde{f}$ and $\tilde{\chi}_1^0\tilde{\chi}_1^0$ productions are also studied as the same as the $\tilde{\chi}_1^+\tilde{\chi}_1^-$ production. No excess was found in these various topologies.

3 LSP Gluino serach

Gluino (\tilde{g}) is heavier than uncoloured gauginos in general SUSY models because of the large value of α_s . But the gluino (\tilde{g}) could be light and stable in some special SUSY braking models. DELPHI reports results on such a light \tilde{g} using data at M_Z -pole.

Since \tilde{g} carries colour charge, the stable \tilde{g} would hadronize to form R-hadrons (\tilde{R}^\pm and \tilde{R}^0). Charged R-hadron(\tilde{R}^\pm) would give the large energy-loss (dE/dx) in the central tracking system, since β of \tilde{R}^\pm is smaller than standard charged particle. This method is used in study on long-lived heavy particles. Neutral R-hadron(\tilde{R}^0) corresponds to $\tilde{g}g$ - and $\tilde{g}q\bar{q}$ -state. It is important to understand how an \tilde{R}^0 will manifest itself in the detector [?].

Average number of collisions between \tilde{R}^0 and materials in hadronic calorimeters are scaled by factor 9/16 comparing the standard neutral hadron. On average, \tilde{R}^0 should undergo 4.3 collision in DELPHI detector. Furthermore the momentum transfer from \tilde{R}^0 to materials becomes smaller in each collision, since the \tilde{R}^0 is heavy. Figure 10 shows the average energy-loss by \tilde{R}^0 as function of the initial energy of \tilde{R}^0 . As shown in this figure, \tilde{R}^0 deposits some part of their energy to calorimeters, but not all. Experimental signature of \tilde{R}^0 is isolated clusters in hadron calorimeter with some \cancel{E}_T .

DELPHI data ($L=46 \text{ pb}^{-1}$) collected in 1994 at centre-of-mass energy of 91.2 GeV have been used to search for the process $e^+e^- \rightarrow q\bar{q}g \rightarrow q\bar{q}\tilde{g}\tilde{g}$, which is shown in Fig. 11(a). Since \tilde{g} would hadronize to form R-hadrons (\tilde{R}^\pm and \tilde{R}^0), the final event-topologies are the following three types; (1) 2 jets + 2 high dE/dx -tracks (2) 2 jets + high dE/dx -track + isolated cluster + \cancel{E}_T , and (3) 2 jets + two isolated clusters + \cancel{E}_T . The fraction of these three topologies depend on the probability that \tilde{g} would hadronize into \tilde{R}^\pm . No evidence was found, and lower-limit on *gluino* mass is shown in Fig. 11(b). The light gluino whose mass was 2-18 GeV is excluded by this study, and uncovered hole of light gluino around 3-4 GeV has been excluded.

4 Conclusions

Various new particles and phenomena are searched for at LEP using data collected at \sqrt{s} upto 209 GeV. Our analysis are based on “topology-oriented studies” not on “model-oriented”. Almost all the possible topologies are covered, and no excess above 2.5σ was found. Many limits not only on SUSY but also technicolour, 4-th generation fermion, excited leptons and anomalous flavour changing are set with interrelations. Table 3 shows, for example, lower-limits on masses of various SUSY particles in CMSSM.

Table 3: *Lower-limits on mass of SUSY particles in CMSSM. (These values are preliminary.)*

Paricles	lower-limit on Mass (GeV)
$\tilde{\chi}_1^\pm$	98.6 ($\Delta M \geq 3$ GeV) 103.5 ($M_{\tilde{\nu}} \geq 300$ GeV)
$\tilde{\chi}_1^0$	36.7 38.7 ($M_{\tilde{\nu}} \geq 300$ GeV)
\tilde{e}_R	98 ($\Delta M \geq 3$ GeV)
$\tilde{\mu}_R$	94 ($\Delta M \geq 3$ GeV)
$\tilde{\tau}_R$	80 ($\Delta M \geq 10$ GeV)
\tilde{t}_1	93 ($\Delta M \geq 15$ GeV)
\tilde{b}_1	92 ($\Delta M \geq 10$ GeV)

5 Acknowledgements

We particularly wish to thank the SL Division for the excellent operation of the LEP accelerator and thank members of the LEP SUSY working group.

References

- [1] J.H. Christenson *et al*, Phys. Rev. Lett. **13**, 138 (1964).
- [2] M.B. Green, Superstrings and the unification of forces and particles, in: Proc. fourth M. Grossmann Meeting on General Relativity (ed. R. Ruffini, Rome, June 1985), **1**, 203 (North-Holland, Amsterdam, 1986).

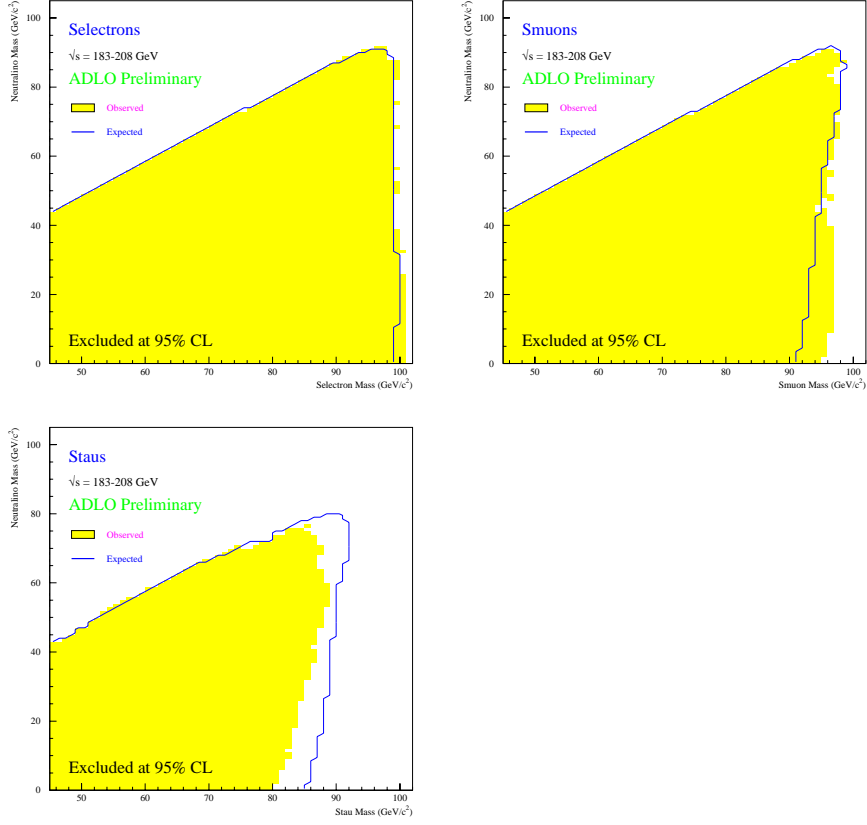


Figure 3: *Excluded regions in $(M_{\tilde{L}_R}, M_{\tilde{\chi}_1^0})$ plane, for $\tan\beta=1.5$ and $\mu=-200 \text{ GeV}$. The hatched regions are excluded by the LEP combined results. The solid lines show the ‘expected’ limits calculated from the sensitivities. (These results are preliminary.)*

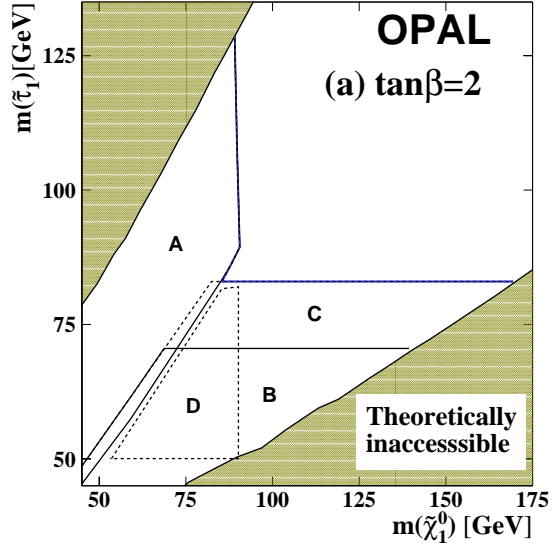


Figure 4: Excluded regions [?] in $(M_{\tilde{\chi}_1^0}, M_{\tilde{\tau}_1})$ plane for $\tan\beta=2$. Each region is exclusively excluded at by (A) $\tilde{\chi}_1^0\tilde{\chi}_1^0 \rightarrow \gamma\tilde{G}\gamma\tilde{G}$, (B) $\tilde{\tau}^+\tilde{\tau}^- \rightarrow \tau^+\tilde{G}\tau^-\tilde{G}$, (C) $\tilde{\mu}^+\tilde{\mu}^- \rightarrow \mu^+\tilde{G}\mu^-\tilde{G}$ and (D) $\tilde{\chi}_1^0\tilde{\chi}_1^0 \rightarrow 4$ lepton final states.

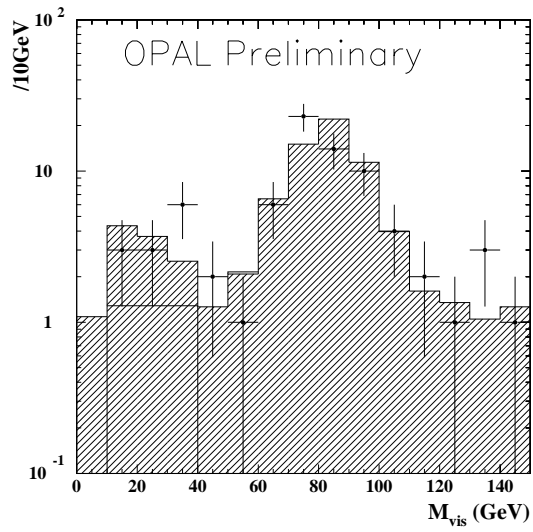


Figure 5: *The distribution of the invariant mass for acoplanar jet pair events at $\sqrt{s}=202\text{-}209$ GeV. The distribution of the data is shown by the points with error bars. Singly-hatched histogram show the predictions from four-fermion processes calculated with *grc4f*.*

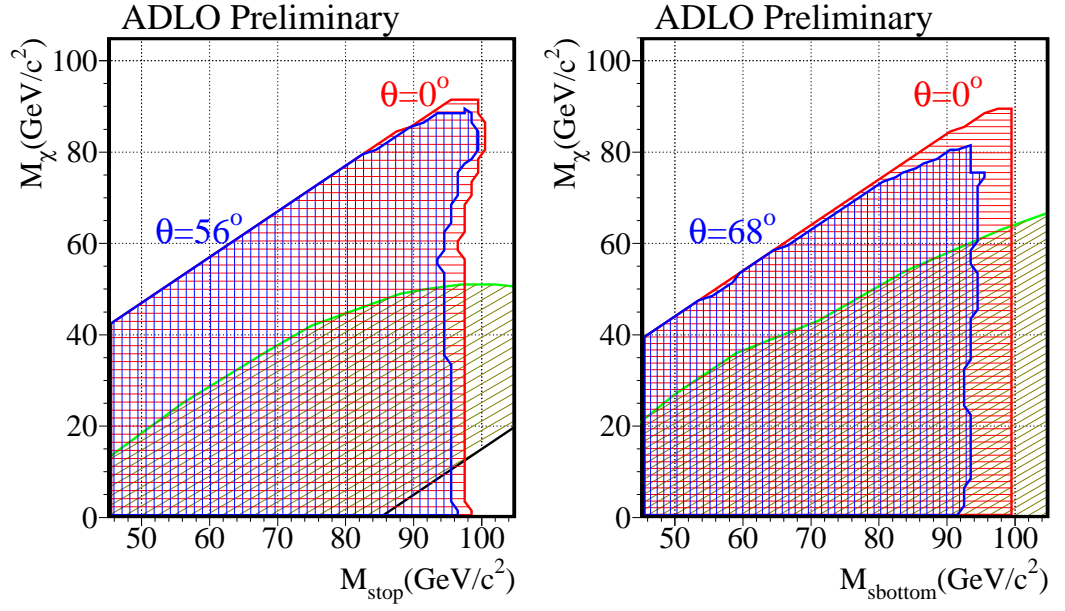


Figure 6: (Left) Excluded regions in $(M_{\tilde{t}_1}, M_{\tilde{\chi}_1^0})$ plane for $\theta_{\tilde{t}}=0$ and 56° . (Right) Excluded regions in $(M_{\tilde{b}_1}, M_{\tilde{\chi}_1^0})$ plane for $\theta_{\tilde{t}}=0$ and 68° . In both figures, the region excluded by the CDF collaboration [?] is also shown with single-hatched area.

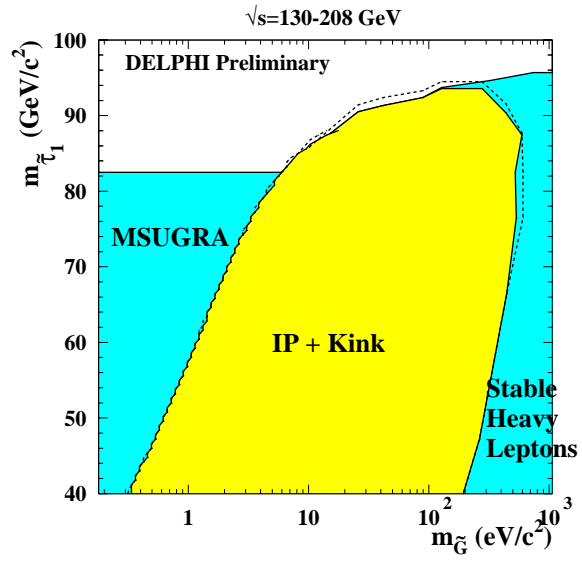


Figure 7: Lower-limit on $M_{\tilde{\tau}_1}$ as function of $M_{\tilde{G}}$ in the GMSB model.

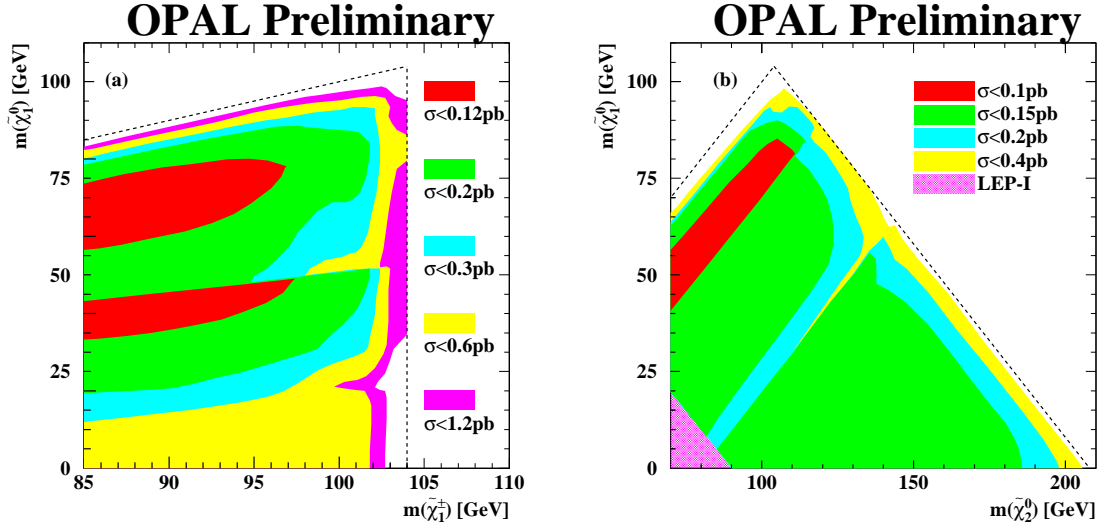
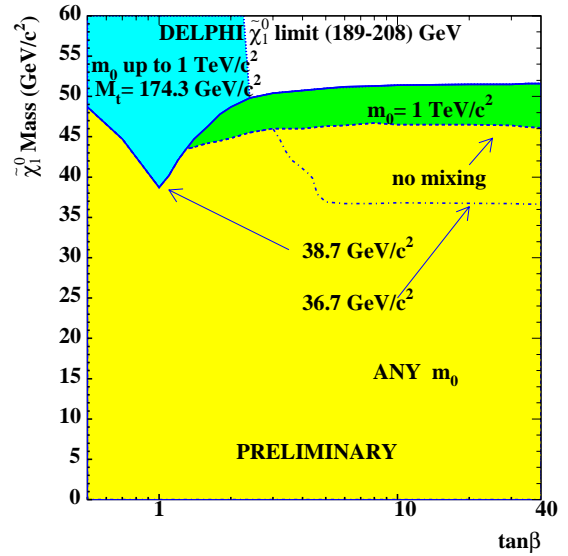
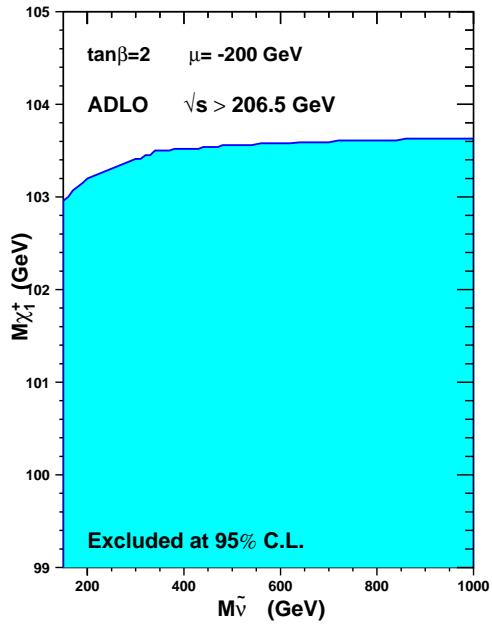


Figure 8: The contour plots of the 95% C.L. upper-limits on the production cross-sections at $\sqrt{s} = 208$ GeV for (a) $e^+e^- \rightarrow \tilde{\chi}_1^+\tilde{\chi}_1^-$ ($\sigma_{\tilde{\chi}_1^+\tilde{\chi}_1^-}$), and (b) $e^+e^- \rightarrow \tilde{\chi}_1^0\tilde{\chi}_2^0$ ($\sigma_{\tilde{\chi}_1^0\tilde{\chi}_2^0}$). The $\tilde{\chi}_1^+$ is assumed to decay into $\tilde{\chi}_1^0 W^{(*)\pm}$, and the $\tilde{\chi}_2^0$ decays into $\tilde{\chi}_1^0 Z^{(*)}$. The kinematical boundaries for $\tilde{\chi}_1^+\tilde{\chi}_1^-$ and $\tilde{\chi}_1^0\tilde{\chi}_2^0$ are shown as dashed lines.



caption (Left) Lower-limit on $M_{\tilde{\chi}_1^\pm}$ as function of $M_{\tilde{\nu}}$ for $\tan\beta=2$ and $\mu=-200$ GeV in the CMSSM. Results in all four experiments are combined. (Right) Absolute lower-limit on $M_{\tilde{\chi}_1^0}$ as function of $\tan\beta$ in the CMSSM. Small $\tan\beta$ is excluded by searches for higgs boson. (DELPHI, Preliminary result)

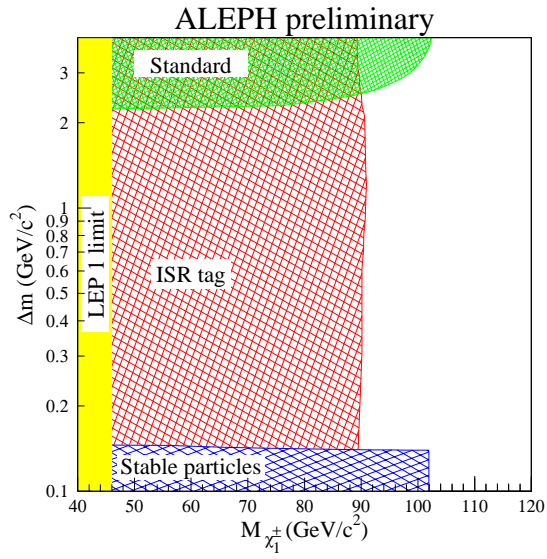


Figure 9: *lower-limit on $M_{\tilde{\chi}_1^\pm}$ as function of mass difference in the CMSSM (Higgsino case). “Standard” indicates study on W^+W^- with \cancel{E}_T topology. (ALEPH, Preliminary result)*

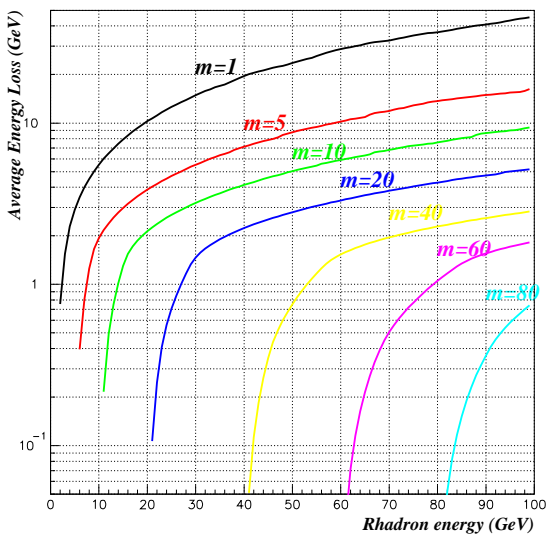


Figure 10: Average energy-loss by \tilde{R}^0 as function of initial energy for various \tilde{R}^0 mass.

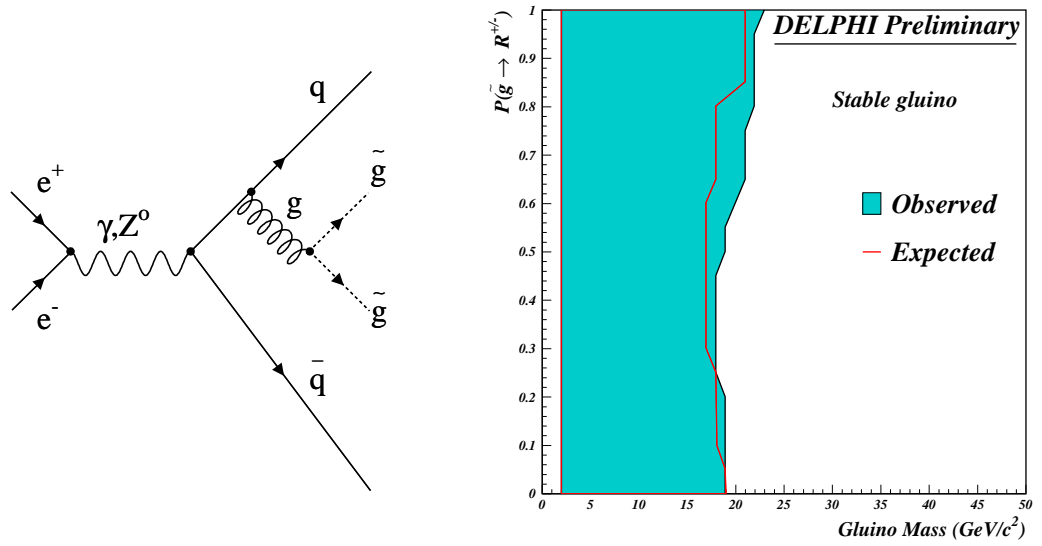


Figure 11: (Left) Feynman diagram of gluon splitting into a pair of gluinos (Right) Excluded regions in $M_{\tilde{g}}$ as the function of the probability that \tilde{g} would hadronize into \tilde{R}^{\pm} .